Article

Sustainably Processed Waste Wool Fiber-Reinforced Biocomposites for Agriculture and Packaging Applications

Parag Bhavsar [1,*], Tudor Balan [2], Giulia Dalla Fontana [1], Marina Zoccola [1], Alessia Patrucco [1] and Claudio Tonin [1]

[1] Institute of Industrial Systems and Technologies for Advanced Manufacturing, Italian National Research Council, Corso Giuseppe Pella 16, 13900 Biella, Italy; giulia.dallafontana@stiima.cnr.it (G.D.F.); marina.zoccola@stiima.cnr.it (M.Z.); alessia.patrucco@stiima.cnr.it (A.P.); claudio.tonin@stiima.cnr.it (C.T.)

[2] Department of Natural and Synthetic Polymers, University "Gheorghe Asachi" of Iasi, Str. Prof. Dr. Doc. Dimitrie Mageron, nr. 28, 700050 Iasi, Romania; balantudorvasile@gmail.com

* Correspondence: parag.bhavsar@stiima.cnr.it; Tel.: +39-0158-493-043

Abstract: In the EU, sheep bred for dairy and meat purposes are of low quality, their economic value is not even enough to cover shearing costs, and their wool is generally seen as a useless by-product of sheep farming, resulting in large illegal disposal or landfilling. In order to minimize environmental and health-related problems considering elemental compositions of discarded materials such as waste wool, there is a need to recycle and reuse waste materials to develop sustainable innovative technologies and transformation processes to achieve sustainable manufacturing. This study aims to examine the application of waste wool in biocomposite production with the help of a sustainable hydrolysis process without any chemicals and binding material. The impact of superheated water hydrolysis and mixing hydrolyzed wool fibers with kraft pulp on the performance of biocomposite was investigated and characterized using SEM, FTIR, tensile strength, DSC, TGA, and soil burial testing in comparison with 100% kraft pulp biocomposite. The superheated water hydrolysis process increases the hydrophilicity and homogeneity and contributes to increasing the speed of biodegradation. The biocomposite is entirely self-supporting, provides primary nutrients for soil nourishment, and is observed to be completely biodegradable when buried in the soil within 90 days. Among temperatures tested for superheated water hydrolysis of raw wool, 150 °C seems to be the most appropriate for the biocomposite preparation regarding physicochemical properties of wool and suitability for wool mixing with cellulose. The combination of a sustainable hydrolysis process and the use of waste wool in manufacturing an eco-friendly, biodegradable paper/biocomposite will open new potential opportunities for the utilization of waste wool in agricultural and packaging applications and minimize environmental impact.

Keywords: superheated water hydrolysis; hydrolyzed wool; kraft pulp; paper/biocomposite

1. Introduction

Traditionally, the paper and board sector has been considered the most economically sensitive sector due to a high consumption of energy and water and its being extensively dependent on the forest ecosystem as a source of wood fibers. As per the Confederation of European Paper Industries report, the European paper and pulp industry delivers a turnover of EUR 90 billion on its competitiveness and sustainable agenda. Based on the EU commission summer economic forecast report 2020, paper and board markets were impacted by a massive decline of −8.3% of the European GDP by global instability due to the COVID-19 crisis; regardless, this is expected to increase by 5.8% in 2021 [1]. Based on the Eurostat report, paper and cardboard were the primary packaging waste materials in the EU, reported to be 31.8 million tons in 2018, followed by plastic and glass [2]. In the EU region, the utilization rate of paper recycling reached 54.6% in 2019, where significant utilization by grade was corrugated and kraft of about 54.2%.

In 2018, the global average consumption of paper was 55 kg per person, while for the EU, it was 124 kg/year/person [3,4]. In the EU region, this industry faces significant challenges of trade barriers, raw material supply, recycling, and rising energy prices. The most significant is a scarcity of raw material resources, primarily due to a mismatch between the raw material's structure and the structure of fiber resources [5,6]. Considering these challenges, clean technologies, sustainable consumption, bioeconomy, and resource efficiency with the introduction of non-wood fibers are the probable solutions to overcoming these crucial challenges. These solutions will ensure efficient production with low waste of resources and minimal environmental impact along with maximizing recyclability and reusability. New advanced, efficient, and abundant resources of non-wood-based fibers from agricultural waste such as straw, hemp, grass, etc.; biomass; non-wood plant species; and low-grade animal fibers can be considered as a profitable and sustainable alternative to overcome the shortage of conventional fibers and reduce deforestation [7–10].

In recent years, many developments have been implemented in the paper industry. Many different types of fillers have been implemented to reduce the proportion of cellulosic fibers, followed by reducing manufacturing cost and environmental concern by reducing the number of trees cut. Along with this, according to statistics, the world's global consumption of paper and paperboard was 422 million metric tons in 2018 [11], and it is projected to increase in the following years [12]. Considering the global need, it is clear that non-wood-based resources will be more important as a raw material for the paper and paperboard industry in the future than today. Previous studies have shown that various agricultural residues such as wheat straw [13], rice straw [14], sunflower stalks [15], sugarcane bagasse [16], oil palm empty fruit brunch [17], etc., and alternative raw materials consisting of tagasaste [18] bridal broom, phragmites [19], giant reed [20], prosopis [21], coniferous [22], leafy wood eucalyptus [23], pine [24], and textile waste [25,26] are considered to be alternative sources for producing pulp and paper sheets.

According to the European Commission regulations on animal by-product control, unserviceable raw wool is classified as a category 3 special waste material. Its collection, storage, transport, treatment, use, and disposal are subjected to EU regulations because of the potential risk to human and animal health. The wool produced in the EU from sheep bred for dairy and meat purposes is of low quality, its economic value is not even enough to cover shearing costs, and it is generally seen as a useless by-product of sheep farming [27], resulting in large illegal disposal or landfilling. However, waste wool finds application in manufacturing carpets, insulating blocks, etc. Wool keratin has been used as a matrix in biocomposites by Savio et al., who produced, in the framework of the FITNESs project, high thermal insulating and sound absorption performance building panels made of 50% recycled sheep wool and 50% technical hemp fibers [28]. In this work, wool and hemp fibers were treated with alkali to produce a bio-based semi-rigid composite panel for thermal and acoustic building insulation. Considering the fact that the wool fiber's exterior scales gave it a hydrophobic property, which makes it unsuitable for the paper industry, other alternative cellulosic fibers such as polyester fibers or polyalkylene carbonate fibers are used in the papermaking process instead of wool [29].

This study provides a new perspective using raw wool fibers in the paper industry with the help of a sustainable hydrolysis treatment with superheated water, an eco-friendly and economical process that uses only water as a solvent. The treatment sterilizes the raw wool at high temperatures, avoiding potential health-related problems ahead of the final application and making it more hydrophilic and biodegradable. No study has been reported until now on the application of superheated water hydrolyzed wool in partial or complete replacement of wood fibers in the paper and boards industry. Therefore, raw wool can play a vital role as it is cheap, readily available, and more sustainable than synthetic biodegradable polymers.

In the agricultural field, mulching films are used to improve microclimate for crop growth by retaining humidity and heat in the soil. They prevent soil erosion and weed development and favor plant development and fruit earliness and quality by decreasing

water demand and herbicide and fertilizer requirements [30]. Most plastic mulches are made of low-density polyethylene (LDPE), the global consumption of which continues to grow worldwide, with an increase of 35% between 2006 and 2017, up to over 2 Mt [31,32]. More than 80.000 km² of agricultural land is covered each year with plastic mulching films [33] for a material cost of 500 EUR/ha without considering labor cost for film laying and removal. Moreover, after its use, non-biodegradable LDPE mulching films contaminated with soil and plant residues have no viable use, and they have to be removed after each cultivation. Removal of residues is laborious, and soil is usually contaminated with plastic particles. Biodegradable plastics have been proposed to decrease the accumulation of LDPE and other persistent plastic wastes in the environment to save time and cost in collecting and managing plastic fragments and avoiding waste generation. The application of hydrolyzed wool/kraft pulp biocomposites in agricultural fields as mulching films will provide essential nutrients, particularly nitrogen, to the soil at the end of each cultivation, and the controlled biodegradation rate is advantageous for the succeeding crop cycle and economically beneficial [34].

In this research, the hydrolysis process with superheated water was implemented to convert the physio-chemical properties of raw wool to make it suitable for biocomposite application. This study provides new insight into the paper/biocomposite industry using sustainability that not only provides economic benefits but also helps to minimize the environmental impact.

2. Materials and Methods

2.1. Material

Raw greasy wool having a fineness of about 25–35 μm was collected from the Piedmont region of Italy. Manual mixing was used to homogenize the wool fibers. For kraft pulp, a commercially available fully unbleached kraft paper from softwood was used to prepare the biocomposites. All the chemicals used were of analytical grade and purchased from Sigma-Aldrich, otherwise explicitly reported.

2.2. Methods

2.2.1. Superheated Water Hydrolysis of Wool

The hydrolysis of raw, greasy wool was carried out in a laboratory-scale reactor specifically designed and built. The reactor can hydrolyze from 0.5 to 3 kg of fibrous material at a maximum temperature of 235 °C (corresponding to an equilibrium pressure of 30 bar); it is equipped with a driving system capable of tumbling material inside the reactor at variable speed. An optimal rotation speed results in homogeneous impregnation of hot water inside the wool fibers in the reactor. In this study, experiments were carried out at a temperature of 140 °C, 150 °C, and 160 °C, corresponding to a pressure of 2.6, 3.8, and 5 bar, respectively, for 60 min. The hydrolysis reactor is supplied with a jacketed electrical heating system. After the hydrolysis treatment, the reactor was cooled down, and the wool hydrolyzates were unloaded and used for further study.

2.2.2. Biocomposite/Paper Preparation

The kraft pulp and the hydrolyzed wool fibers were separately refined on a Jokro mill by applying the SR EN 25264-3:1997 standard method [35]. A refining degree of 27 °SR was measured for the softwood kraft pulp. The three types of hydrolyzed wool fibers were subjected to a refining cycle for 60 s, aimed at reducing their length and their tendency to entangle with each other.

A total of fifteen different paper stock compositions were prepared by mixing the refined softwood kraft pulp with each of the hydrolyzed wool fibers, in water suspensions in different dry weight ratios without addition of filler or any chemical additives (cellulose:wool = 90:10, 80:20, 70:30, 60:40, and 50:50). Laboratory sheets with a basis weight of 60 g/m² were obtained on a Rapid-Kothen former according to the ISO 5269-2:2004 standard method [36].

2.3. Characterization

2.3.1. Scanning Electron Microscopy (SEM)

Morphological investigations on samples were carried out by an LEO 135 VP Scanning Electron Microscope (SEM) (Leica Electron Optics, Rome, Italy) with an acceleration voltage of 15 kV, 50 pA of the current probe, and 30 mm working distance. The samples were mounted on aluminum specimen stubs with double-sided adhesive tape. Samples were sputter-coated with a 20–30 nm thick gold layer in rarefied argon, using a sputter coater with a current of 20 mA for 4 min.

2.3.2. Fourier Transform Infrared Spectroscopy (FT-IR)

The Fourier transform infrared spectroscopy (FT-IR) spectra of greasy wool, wool hydrolyzates, and biocomposite/paper were recorded on a Nexus Thermo Nicolet Spectrometer (Milan, Italy). The spectra were obtained with 100 scans, in the range 650–4000 cm^{-1} with a resolution of 4 cm^{-1} and a gain of 8.0.

2.3.3. Tensile Strength

Tensile testing was measured in a conditioned standard atmosphere at 20 °C, 65% relative humidity (RH) with an Instron 5500 R Series IX Dynamometer (Turin, Italy), according to the T 494 om-96 standard (tensile properties of paper and cardboard). Films were cut into strips 5 mm width $\times$ 20 mm length and submitted to tensile stress at a constant rate of 10 mm/min. At least three samples were measured for tensile strength, elongation at break, and tensile energy absorption, reporting the average results.

2.3.4. Differential Scanning Calorimetry (DSC)

DSC analysis was performed with a Mettler Toledo DSC 821 (Milan, Italy) calorimeter calibrated by an indium standard. The calorimeter cells were flushed with 100 mL min^{-1} nitrogen. The runs were performed on conditioned samples (20 °C, 65% RH for 24 h) from 25 to 500 °C, at a heating rate of 10 °C min^{-1}.

2.3.5. Thermogravimetric Analysis (TGA)

TGA was performed with a Mettler Toledo TGA 850 analyzer (Milan, Italy). The temperature range was from 25 to 500 °C with a heating rate of 5 °C min^{-1} in a nitrogen atmosphere. About 3 mg of sample was used in each test using Al_2O_3 crucibles. The data were collected on a computer with the Mettler Toledo STARe System.

2.3.6. Biodegradation Testing in Soil

Hydrolyzed wool/kraft pulp biocomposites made of different compositions were cut into 5×5 cm^2 pieces, weighed, and placed into nylon mesh bags. Four replicates of each sample for each time point were then buried under 15 cm of soil in the CNR STIIMA Biella field plot and then were removed from the ground at 30, 60, and 90 days of interval. During these weeks, in which there was little rain, the plot was sprinkled with water. After removal, samples were gently cleaned with a brush, conditioned for 24 h at 20 °C and 65% (RH), weighed, and tested. The mass was weighed with an analytical balance, and the weight loss (W) was calculated using Equation (1). To reduce the error, the weight loss ratio was determined as the mean value of four samples.

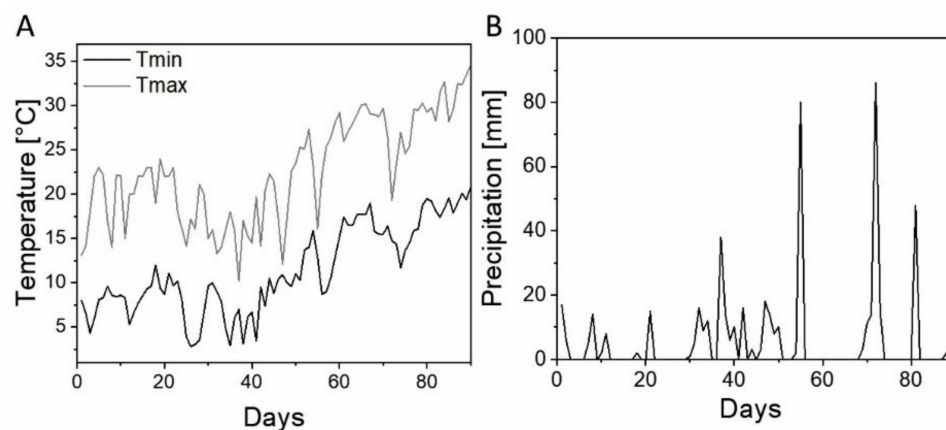$$W = \frac{(Mi - Md)}{Mi} \times 100\% \tag{1}$$

W = Weight loss of the biocomposite after *X* days (%).
Mi = Initial mass of the biocomposite (g).
Md = Final mass of the bio composite after *X* days of degradation (g).
* *X* = 30, 60, 90 days.

Average outdoor temperatures were about 11.3 °C min and 22.6 °C max over the 3 months of the experiment. Rainfall was very light, and the average rainfall of 90 days was 5 mm [37,38] as shown in Figure 1.

Figure 1. Ambient average temperatures and precipitation were recorded in Biella, Italy, during field trials of biocomposite biodegradation. (**A**) Indicates Tmin and Tmax temperatures in °C, and (**B**) precipitation in millimeters. (Data obtained from Archivio meteo storico, Biella, Italy, 3B meteo).

3. Result and Discussion

3.1. Scanning Electron Microscopy (SEM)

The morphology of biocomposites made of different compositions using kraft pulp and wool hydrolyzed at varied temperatures, studied at different magnifications, are shown in Figure 2, and their biodegradation in the soil at the end of 30, 60, and 90 days is shown in Figure 3. The SEM micrograph in Figure 2a represents the surface and cross-section of the control 100% kraft pulp-based biocomposite. All the hydrolyzed wool samples obtained at different temperatures were dried in an oven at 50 °C. Microscopic investigations by SEM in Figure 2c–e show the fiber structure of wool samples with different surface morphology based on the effect of temperature during the hydrolysis treatment. In the sample treated at 160 °C, wool fibers still retain their elongated shape morphology, but cuticles are completely removed, while most fibers show no cuticular layer and are morphologically more damaged. The appearance of fibers is sticky in nature in their relation to one another because of foreign materials or hydrolyzed wool proteins. The wool fiber hydrolyzed at 150 °C shows less damaged fibers in comparison with the 160 °C hydrolyzed wool fibers, while the fibers generally have a bent, twisted morphology with fragile breaks. The fibers shown in the SEM image (d) are more bent than the normal wool fiber. In the wool fibers hydrolyzed at 140 °C, the appearance of wool fiber shows morphological characteristics of wool with cuticular scales intact with minor damage. The fracture of wool fiber is smooth; this indicates the brittleness of the treated fibers.

The SEM micrographs of a biocomposite made of 100% kraft pulp in Figure 2f and a 50%-50% kraft pulp and hydrolyzed wool shown in Figure 2g–i, respectively, show the distribution, appearance, and compactness of fibers within the biocomposite structure. The SEM micrograph of 100% kraft pulp shows a compact structure where cellulose fibers are densely attached with each other in hydrogen bonding without any gap in the structure. In contrast, the micrograph (i) of 160 °C hydrolyzed wool fibers incorporated with cellulose fibers shows similar characteristics where fiber structure is compacted and bonded with hydrogen bonding between cellulose and wool fibers, as wool fibers were transformed into more hydrophilic characteristics after the hydrolysis treatment. Furthermore, the sticky glue-like characteristics of wool protein hydrolyzate from hydrolyzed wool fibers led to improved fiber bonding inside the biocomposite. Similarly, SEM micrographs (g) and (h) also show hydrolyzed wool fiber entrapment and compactness within the kraft cellulose fibers. In general, the hydrolysis treatments of wool fibers led to fiber swelling,

hydrophilicity, and cracking and made the wool fiber soft and flexible, resulting in increased surface area with groovy characteristics of the hydrolyzed fiber due to damage or removal of external cuticle structure, which increases fiber bonding and contributes to a certain mechanical strength.
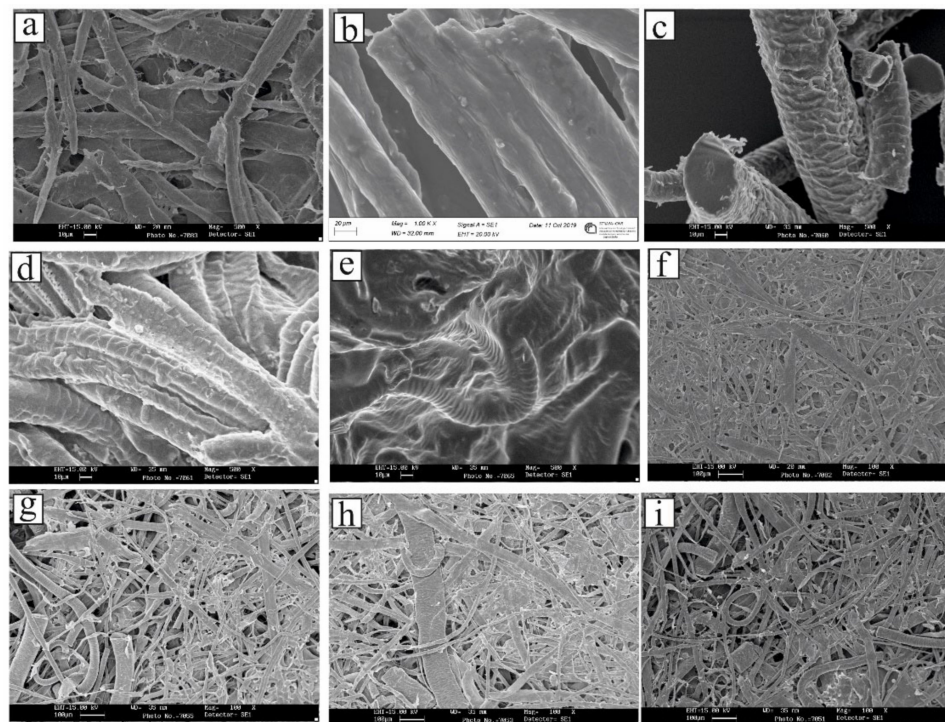
Figure 2. SEM analysis of (**a**) kraft pulp (500×); (**b**) raw wool (1000×); (**c**) 140 °C hydrolyzed wool (500×); (**d**) 150 °C hydrolyzed wool (500×); (**e**) 160 °C hydrolyzed wool (500×); (**f**) control 100% kraft pulp biocomposite (100×); (**g**) 50%-50% kraft pulp/140 °C hydrolyzed wool biocomposite (100×); (**h**) 50%-50% kraft pulp/150 °C hydrolyzed wool biocomposite (100×); (**i**) 50%-50% kraft pulp/160 °C hydrolyzed wool biocomposite (100×).

The surface morphology of 100% kraft pulp and mixed composition of fibers in biocomposite was examined using SEM images to confirm the increased resistance against biodegradation. In 100% kraft pulp biocomposite, a significant fiber degradation was found after 30 days Figure 3a in comparison with initial fiber surface morphology in Figure 2a. As shown in Figure 3a, after 30 days of soil burial, the kraft pulp cellulose fibers formed mainly longitudinal, and, in particular, diagonal cracks formed, a phenomenon that has already been described [39–41]. The diagonal splitting can be related to the crystalline or more resistant portions of cellulose fibers that are frequently positioned at an angle to the fiber axis [39]. Longitudinal fibrillation may develop because the interior of the fibers, which is exposed as the outer layer degrades, carries alternating ridges and cavities that may be caused by microorganisms [42,43]. After 60 days of soil biodegradation, the surface morphology of 100% kraft pulp cellulose fibers was prone to an advanced stage of biodegradation where fibers appeared to be in a shapeless form and to be morphologically more damaged. Finally, at the end of 90 days, microbial activity from the soil on cellulose fibers might significantly influence the external and internal layers of the fibers. It appears that the splitting of the fiber surface is a mark of early deterioration, and further degradation is indicated by erosion, bisection, and groove/ridged surface appearance, as seen in Figure 3c. In general, in hydrolyzed wool/kraft pulp biocomposite, the wool fibers seem to be more resistant to biodegradation than cellulosic fibers depending on hydrolysis temperature. The SEM micrographs of biocomposites consisting of hydrolyzed wool fibers after 90 days show colonies of microorganisms on the surface of the fibers. The presence of microorganisms leads to long cavities extending deep within the fibers that were created

and inhabited by microorganisms, mainly seen in Figure 3f,l. Similar effects were also observed by Broda et al. [44].
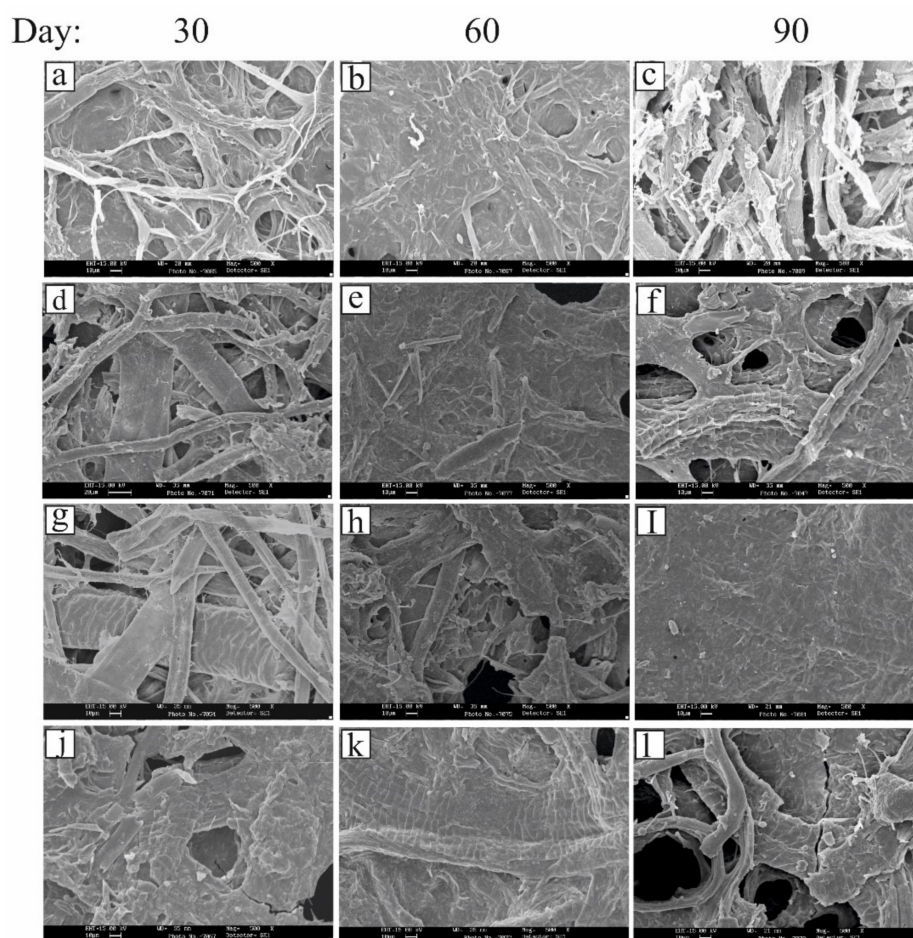
Figure 3. SEM analysis at 500× magnification of kraft pulp/wool hydrolyzed bio composite after 30, 60, and 90 days of soil biodegradation: 100% kraft pulp biocomposite after (**a**) 30 days, (**b**) 60 days, and (**c**) 90 days; 50%-50% kraft pulp/140 °C hydrolyzed wool biocomposite after (**d**) 30 days, (**e**) 60 days, and (**f**) 90 days; 50%-50% kraft pulp/150 °C hydrolyzed wool biocomposite after (**g**) 30 days, (**h**) 60 days, and (**i**) 90 days; 50%-50% kraft pulp/160 °C hydrolyzed wool biocomposite after (**j**) 30 days, (**k**) 60 days, and (**l**) 90 days.

While in the case of 100% kraft pulp biocomposites, many fibers with distinct fibrils weakly linked were observed, as shown in Figure 3c, in the humid environment, the microorganisms developed in the soil led to the secretion of enzymes and utilized the wool as a source of nutrients. The primary evidence of the degradation of the mixed fiber biocomposite was observed to be holes, as seen in Figure 3d–l; a similar phenomenon was also observed by Jewell and Dimbleby (1966) [45]. In Figure 3d,g,j, in the biocomposite made of hydrolyzed wool fiber at 140 °C, 150 °C, and 160 °C and kraft pulp after 30 days of soil degradation, the surface morphology of fibers appeared to be in the form of shapeless aggregates (except at 140 °C hydrolyzed wool-based biocomposite) and to be morphologically more damaged, where peeling of outer scale layers, partial erosion, cracks, and holes are prominently visible, as evidenced by other authors in the literature [41,44,46,47]. At the end of 60 and 90 days of soil degradation, as shown in Figure 3e,f,h,i,k,l, hydrolyzed wool and cellulose fibers appeared to be fused with each other, and shapeless aggregates were observed. The undulated appearance of the wool fibers shown in Figure 2d–l could be attributed to degradation [48,49].

Based on prior studies on the soil degradation mechanism of cellulose, both cellulolytic and lignolytic enzymes are produced by soil bacteria, actinomycetes, and fungi. Fungi are particularly active in the biodegradation of cellulose, hemicellulose, and lignin, primarily those belonging to the Basidiomycetes, Ascomycetes, and Fungi imperfecti. Most organisms prefer cellulose substrates that are amorphous or low in molecular weight, even though as a single carbon source, some soft-rot Basidiomycetes, such as Trichoderma sp., are able to use crystalline cellulose [50]. Because of the insolubility of cellulose in water, enzyme reactions are performed outside the microbial cell through enzymes secreted by the organisms. Endocellulase, exocellulase, and β-glucosidase are believed to act in sequence and co-operation to bring about the biodegradative hydrolysis of cellulose [51,52].

Previous studies have shown two mechanisms in wool fibers, namely surface erosion and radial penetration of wool fiber by microbes [53,54]. The first mechanism shows that the wool is gradually degraded from the exterior cuticles to the inner cortex. The initial attack is on the cell membrane complex and the cytoplasmatic residue. Degradation then further proceeds with the enzyme invasion of endocuticle and inter macro fibrillary matrix [53]. The cell membrane complex and the inter macro fibrillary matrix are destroyed, leading to loss of the exterior cuticle and separation of certain cortical cells. As a result, cortical cells lose their cohesiveness, and the removal of amorphous proteins that fill the inter macro fibrillary gap causes defibrillation of fibers. Individual macro fibrils are observed to be separated and then destroyed at this step.

The release of keratinolytic enzymes by the fungi penetrating organs occurs in the second mechanism, reflecting an early stage of fungal attack. Deep holes perpendicular to the fiber axis are developed by the enzyme activities [55].

In this study, the SEM micrographs confirm the similar fiber destruction mentioned in the above mechanism, where gradual degradation of fibers occurs from the cuticle to the cortex, with subsequent fiber fibrillation in some cases. Aside from this, slow, progressive biodegradation is seen in the majority of fibers.

3.2. Fourier Transform Infrared Spectroscopy (FT-IR)

FTIR spectra of wool and hydrolyzed wool treated for different temperatures are shown in Figure 4b–e. The FTIR spectra show that the hydrolysis treatment does not result in any new chemical groups or free residues in wool. The FTIR spectra of wool and hydrolyzed wool fibers show classical band absorptions in the three different regions, namely amide I, amide II, and amide III, which are the strongest absorption bands of proteins. The stretching vibrations of the C=O bond are attributed to the absorption frequency of amide I (1630–1650 cm^{-1}). Amide II is observed in the 1530–1550 cm^{-1} range and attributed to the bending vibrations of N–H bonds. Amide III is responsible for the absorption frequency in the range of 1220–1240 cm^{-1}. C=O and N–H bonds take part in hydrogen bonding [56,57]. At 3282 and 3065 cm^{-1}, respectively, the absorption frequency of amide A and amide B corresponds to the N–H vibrations. The C–H stretching is attributed to the absorption bands in the range of 2800–3000 cm^{-1}. The stretching vibration of O–H and N–H bonds is responsible for the broad absorption band in the 3200–3500 cm^{-1} range.

In comparison with the original wool fibers, some changes in the absorption band intensity are observed in hydrolyzed wool fibers, mainly in the range of 1100–1700 cm^{-1}. Compared with the original wool, sharp absorption bands are observed in the range of 2850–2965 cm^{-1} attributed to C–H stretching. Wool fiber's disulfide bonds contribute significantly to its physical and chemical characteristics. The variations observed in the region 1000–1300 cm^{-1}, attributed to different sulfur-containing chemical groups of wool that comprise the oxidative disulfide intermediates and the amide III band, are consistent with disulfide bond modification because of hydrolysis treatment. In the hydrolyzed wool samples, the wedge-shaped peaks of amide I 1650 cm^{-1} and II 1530 cm^{-1} were detected. The bond breakage due to the hydrolysis process may be responsible for transforming smooth amide peaks of original wool into wedge shape peaks [58]. Changes in peak

intensity and positions in the amide group are attributed to changes in wool keratin structure.
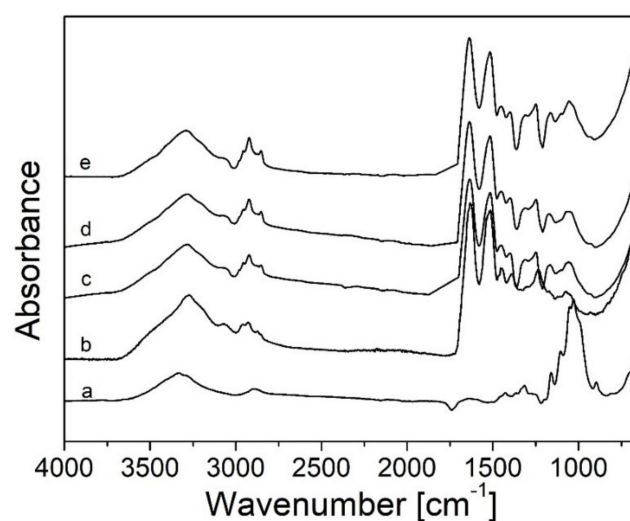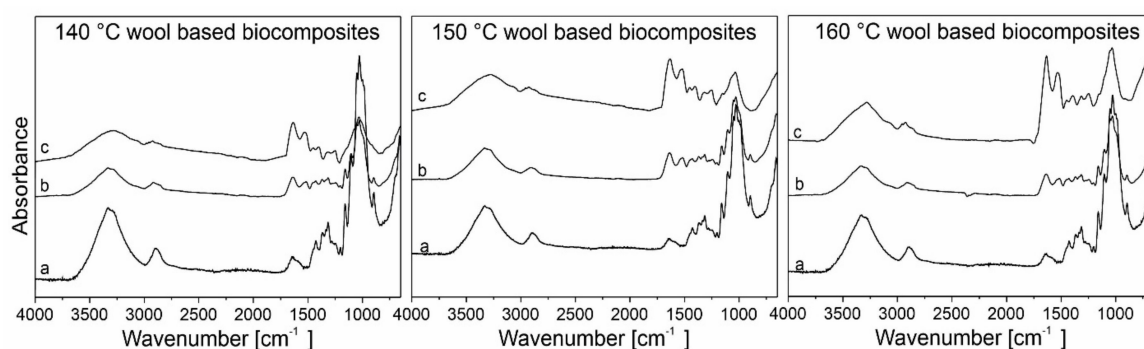

Figure 4. FTIR spectra of original wool, superheated water hydrolyzed wool, and kraft cellulose pulp: (**a**) 100% kraft cellulose pulp; (**b**) original wool; (**c**) 140 °C hydrolyzed wool; (**d**) 150 °C hydrolyzed wool; (**e**) 160 °C hydrolyzed wool.

In the FTIR spectra of kraft pulp cellulose fibers in Figure 4a, two information-rich areas of absorption bands in the range of 2800–3800 cm^{-1} and 840–1800 cm^{-1} are mainly observed, where absorption bands in the range of 3000–3800 cm^{-1} are attributed to the OH stretching and bending vibration of cellulose, while other regions, which are also termed as the fingerprint zone, are attributed to the different stretching vibrations of cellulosic groups. The peaks observed in the range of 2800–3000 cm^{-1} correspond to CH stretching; this area is less analyzed due to similar peaks observed for hemicellulose, cellulose, and lignin [59–62]. In the range of 1633–1650 cm^{-1}, the absorption frequency attributed to the H–O–H bending is due to the water molecule's absorption. The peaks observed in the 1420–1430 cm^{-1} range correspond to symmetric bending of CH_2 of cellulose. The absorption band at 1330–1380 cm^{-1} is attributed to the bending vibrations of the polysaccharide C–H and C–O groups [63,64]. The C–O–C asymmetric stretched vibrations associated with cellulose I and cellulose II have been attributed with absorption bands in the range of 1161 cm^{-1} [65]. The bands at 1105 cm^{-1} and 1029 cm^{-1} are attributed to the glucose ring asymmetric stretching and C–O stretching. In the spectra of kraft pulp cellulose fibers, the lignin-associated bands at 1600, 1510, and 830 cm^{-1} are absent. These bands are attributed to aromatic skeletal vibrations and C–H out-of-plane vibration lignin [66]. The increase in peak intensities in the acquired spectra around 900 cm^{-1} might be due to interactions between glycosidic linkages and cellulose glucose units [67].

Figure 5 represents the FTIR of hydrolyzed wool/kraft pulp biocomposite subjected to the soil degradation after 0 and 90 days, where wool was hydrolyzed at three different hydrolysis temperatures (140 °C, 150 °C, and 160 °C). All the samples that undergo soil degradation show significant changes in the peak intensities after 90 days of biodegradation; both for hydrolyzed wool and kraft cellulose, fibers are visible in the above figure. In Figure 5, sample (a) represents the 100% kraft pulp cellulose fiber composite, while (b) represents the mixed fiber composite, where significant presence of amide I and amide II confirms the presence of hydrolyzed wool in biocomposite, which will be helpful for comparing the changes in peak intensities after soil degradation. In the FTIR of mixed fiber biocomposites, before biodegradation, the spectra show higher peak intensities. The peak intensities are attributed to kraft cellulose pulp and hydrolyzed wool in the region of 2900–3500 cm^{-1} and 1500–1800 cm^{-1}, which is mainly due to OH stretching and the bending vibration of cellulose and amino acids present, corresponding to amide hydrogen and hydroxyl groups,

respectively. After biodegradation, the FTIR of all biocomposites revealed a substantial reduction in peak intensities. These changes in the peak intensities after soil degradation indicate that initial functional groups in the hydrolyzed wool fibers were attacked by soil microorganisms through hydrocatalytic enzymatic process, converting them into water soluble compounds that the microbes may easily absorb and convert into new biomass. Due to the presence of cellulosic fibers in the biocomposite, the breakage of the OH bonds, methyl and methylene of cellulose, which happens due to soil microorganisms attacking the cellulose chain, is responsible for reducing peak intensities at 3500 and 2900 cm^{-1}. As seen in Figure 5, changes in the peaks belong to cellulosic fibers, particularly 1161 cm^{-1} attributed to the C–O–C asymmetric vibration; 1105 cm^{-1} corresponding to glucose ring asymmetric stretching; and 1030 and 1053 cm^{-1} belonging to C–O stretching, were found to be absent after 90 days of degradation due to enzymatic degradation [68]. However, in some mixed fiber spectra after 90 days of soil burial, testing resulted in increased peak intensities, particularly in the region of 1500–1700 cm^{-1} bands, which can be attributed to carbonyl groups, absorbed water, and amide I and II. The changes in peak intensities result from a higher percentage of wool at the time of testing in biocomposite because of slow degradation of hydrolyzed wool compared with the cellulosic fibers showing a strong intensity peak, which are observed to be reduced again in soil burial samples tested for 90 days.

Figure 5. FTIR spectra of kraft pulp biocomposite, superheated water hydrolyzed wool, and kraft cellulose pulp biocomposite and biodegradation after 90 days: (**a**) 100% kraft cellulose pulp biocomposite; (**b**) 50%-50% Kraft pulp/hydrolyzed wool biocomposite after 0 days (**c**) and 90 days, respectively.

3.3. Tensile Strength

The mechanical property of kraft pulp/hydrolyzed wool biocomposite is expressed in tensile index, tensile energy absorption, and elongation at break shown in Figure 6. In the case of 100% kraft pulp biocomposite, the tensile index resulted in a higher strength of about 56.19 Nm/g in comparison with mixed fiber biocomposite due to better fibrillation and fiber-to-fiber bonding in kraft pulp cellulosic fibers. As shown in Figure 6, in general, as the percentage of hydrolyzed wool starts to increase in the biocomposite, and there is a gradual decrease in strength. This might be due to the fact that hydrolyzed wool fibers and wood pulp fibers have less hydrogen bonding energy. This is partly due to the strength of the fibers themselves, but most of the dry strength comes from the bonding between the individual fibers [69–71]. A tensile index comparison within the biocomposite made of hydrolyzed wool at 140–160 °C shows that the effect of hydrolysis temperature plays a significant role. The biocomposite made from 140 °C and 150 °C hydrolyzed wool performed better in comparison with the 160 °C; this may be attributed to a higher temperature of hydrolysis that increased the intensity of making or breaking of chemical bonds, such as disulfide linkages and peptide bonds by water directly or induced by water, which resulted in a reduction of the strength of wool fibers. This is supported by changes in wool fiber morphology due to the extent of the hydrolysis temperature, which is visible in SEM morphographs.
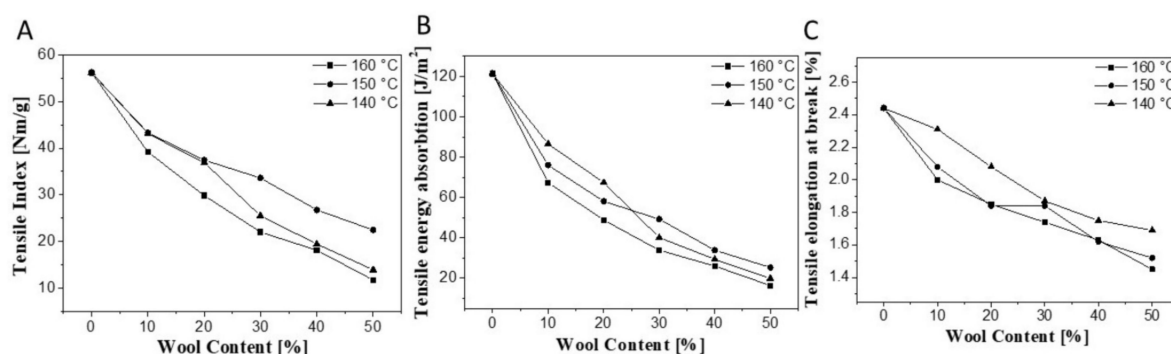
Figure 6. Tensile index (**A**), tensile energy absorption (**B**), and elongation at break (**C**) of 100% kraft cellulose pulp biocomposite (0% wool content) and kraft cellulose pulp/hydrolyzed wool at different hydrolyzed temperatures with 10–50% of wool content in biocomposite.

In comparison with 100% kraft pulp biocomposite, the tensile index of biocomposite containing hydrolyzed wool processed at 140 °C decreases from 23 to 75%, 150 °C decreases from 22 to 60%, and 160 °C decreases from 30 to 79%, as the hydrolyzed wool percentage increases from 10 to 50%, respectively. The tensile energy absorption (TEA) of kraft pulp/hydrolyze wool biocomposite was observed to be reduced considerably as the content of hydrolyzed wool increased in the biocomposite. In comparison with 100% kraft pulp biocomposite, the tensile energy absorption of biocomposite containing hydrolyzed wool processed at 140 °C decreases from 28 to 83%, 150 °C decreases from 37 to 79% and 160 °C decreases from 44 to 86% as the hydrolyzed wool percentage increases from 10 to 50%, respectively. This shows that the energy necessary to break the kraft pulp/hydrolyzed wool fiber biocomposite is less than the energy required to rupture the 100% kraft pulp biocomposite. These results indicate that additional research is needed to enhance the tensile characteristics of the kraft pulp/hydrolyzed wool fiber biocomposite. With the help of different hydrolyzed wool pulp preparation procedures and chemicals such as binder materials or crosslinking molecules, biocomposites' weak points and flaws may be reduced. The difference in the properties of hydrolyzed wool and kraft pulp influenced the elongation at break of biocomposite. This leads to a decrease in elongation at break from 2.39 to 1.69% of 140 °C, 2.08 to 1.52% of 150 °C, and 2 to 1.45% of 160 °C processed hydrolyzed wool containing biocomposite in comparison with 2.44 of 100% kraft cellulose pulp biocomposite. All of the samples have an elongation at break values of less than 2%, with no distinct variation between them. In general, differences in the mechanical properties of biocomposites with hydrolyzed wool content could be due to differences in fiber characteristics such as density, fiber cohesion force, and non-uniform fiber distribution.

3.4. Differential Scanning Calorimetry (DSC)

The DSC curves of samples hydrolyzed at 150 °C (100% hydrolyzed wool, 50%-50% kraft pulp/hydrolyzed wool, 70%-30% kraft pulp/hydrolyzed wool, 90%-10% kraft pulp/hydrolyzed, and finally 100% kraft cellulose) are reported in Figure 7.

In each thermogram, the first endotherm peak below 100 °C is associated with water evaporation. The hydrolyzed 100% wool shows a bimodal endothermic peak in the range between 200 and 340 °C, at 215 °C due to the denaturation of α-form crystalline regions, and about 275 °C due to the degradation of highly cross-linked (disulfide bonds) inter-macrofibrillar matrix keratins [72–74]. The sample with 50%-50% kraft pulp/hydrolyzed wool (line b) also shows the same peak; in the other samples with less wool, this instead becomes imperceptible, and the peak is related to the pyrolysis of cellulose occurring at 360 °C [75,76].
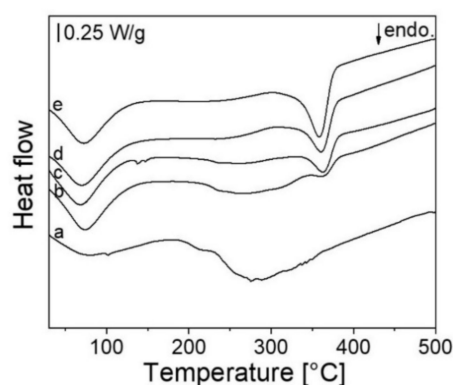
Figure 7. DSC curves of samples at 150 °C: (**a**) 100% hydrolyzed wool; (**b**) 50%-50% kraft pulp/hydrolyzed wool; (**c**) 70%-30% kraft pulp/hydrolyzed wool; (**d**) 90%-10% kraft pulp/hydrolyzed; and finally (**e**) 100% kraft cellulose.

3.5. Thermogravimetric Analysis (TGA)

The TG curves and their first derivatives of samples at 150 °C (100% hydrolyzed wool, 50%-50% kraft pulp/hydrolyzed wool, 70%-30% kraft pulp/hydrolyzed wool, 90%-10% kraft pulp/hydroly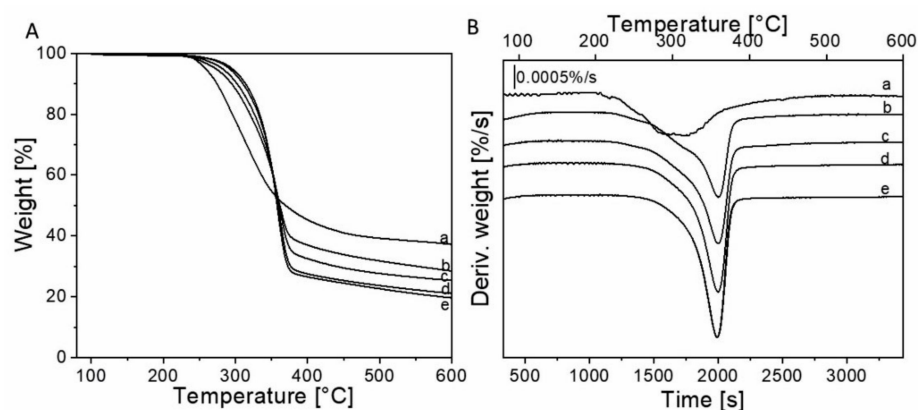zed, and finally 100% kraft cellulose) are shown in Figure 8A,B, respectively. The weight loss percentage in the 100% hydrolyzed wool (line a) corresponds to the weight loss (60 wt% at 600 °C) due to the decomposition/denaturation of the protein fiber structure [74].

Figure 8. TG curves of samples (**A**) and their first derivatives (**B**) at 150 °C: (**a**) 100% hydrolyzed wool; (**b**) 50%-50% kraft pulp/hydrolyzed wool; (**c**) 70%-30% kraft pulp/hydrolyzed wool; (**d**) 90%-10% kraft pulp/hydrolyzed; and finally (**e**) 100% kraft cellulose.

The first derivative graph shows that the mixed samples have two different degradation rates, the first one at 300 °C due to the decomposition of wool and the second one associated with cellulose pyrolysis with the maximum weight loss rate attained at 360 °C. Increasing the concentration of cellulose increases the thermal degradation; indeed, the sample with 100% kraft cellulose has a weight loss of 77%, while the sample with 50%-50% kraft pulp/hydrolyzed wool is 67% [77].

3.6. Biodegradation Testing in Soil

Visual appearance of samples prior and after biodegradation testing in soil is shown in Figure 9. The timespan of soil burial testing was initiated from March to June, where biodegradation of biocomposites occurred. The average temperature of 22.6 °C and rainfall of 5 mm were recorded over a 90-day time span. The biocomposites entrapped in the soil are exposed to microorganisms that secrete enzymes and disrupt the disulfide bonds in the hydrolyzed wool fiber and cellulose, hemicellulose, and lignin. The breakdown of

these bonds resulted in the breaking of crosslinking between the cellulosic and hydrolyzed wool fiber bonds or between the different parts of the same protein or cellulosic fiber chains, which are responsible for stabilizing fiber structure. The hydrolysis of wool fiber resulted in disruption of disulfide bonds in wool fiber, which was more readily available to microorganisms for breakdown and provides easy access to intact peptide links that were resistant to degradation, leading to the disintegration of wool keratin. Initially, keratin breakdown occurred in the outer cuticle, which has a greater cysteine concentration than the whole fiber [78]. The disintegration of wool keratin leads to significant damage to the fiber surface and cuticle cells, subjected to erosion of scales observed in terms of weight loss and visible after 30 days of soil burial testing.
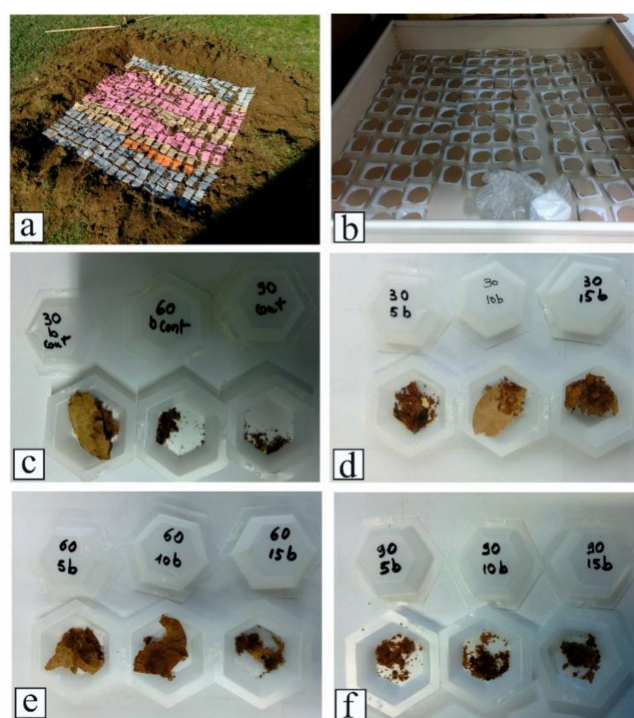
Figure 9. Soil burial degradation of (**a**) visual appearance of samples prior to field testing; (**b**) control samples use for field study; (**c**) 100% kraft pulp biocomposite samples after 30, 60, and 90 days; (**d**) 50%-50% 140 °C, 150 °C, and 160 °C hydrolyzed wool and kraft pulp biocomposite samples after 30 days; (**e**) 50%-50% 140 °C, 150 °C, and 160 °C hydrolyzed wool and kraft pulp biocomposite sample after 60 days; (**f**) 50%-50% 140 °C, 150 °C, and 160 °C hydrolyzed wool and kraft pulp biocomposite sample after 90 days of soil burial testing.

Furthermore, enzyme leads to biodegradation of the cuticle layer, and, at the same time, enzyme reached the core of the fibers causing the following disruption in the deeper layers of cortical cells. This weakened the tight structure of the core, and fibrillation began. The later breakdown of disulfide crosslinks by the enzyme secreted by microorganisms leads to disruption of peptide linkages in the keratin chains, resulting in the removal of material between the inter macrofibrillary spaces, leading to fibrillation. The disruption of the cuticle, cortical cell layers, and fibrillation leads to the weakening of fibers and affects their mechanical properties.

The biodegradability of biocomposites is assessed by evaluating the weight loss (%) of 100% kraft pulp and mixed fiber composites after 30, 60, and 90 days of degradation, as shown in Table 1; the representative surface morphology was shown in Figure 6. As can be seen in Table 1, the biodegradability of the mixed fiber composite material samples increases with increasing the residence time in soil. Moreover, three samples resulted in 100% degradation after 90 days. The percentage of weight loss in all biocomposites is directly proportional to the number of days of soil burial. The hydrolysis treatment of wool

fiber resulted in comparative degradation with respect to 100% kraft pulp biocomposite, which indicates that hydrolysis with superheated water plays an essential role in controlling the biodegradation of wool, and it has been experimentally demonstrated that the biocomposites produced using this process are entirely biodegradable and compostable.

Table 1. Weight loss percentage of the biocomposites obtained after 30, 60, and 90 days of degradation in soil.

No.	Biocomposite Composition	Weight Loss %		
		30 days	60 days	90 days
Control	(100% kraft pulp)	12.85	64.30	(~100)
1	(160 °C 90:10)	14.60	67.86	93.90
2	(160 °C 80:20)	20.40	83.49	93.47
3	(160 °C 70:30)	34.25	72.25	89.89
4	(160 °C 60:40)	41.14	67.34	97.29
5	(160 °C 50:50)	31.52	78.27	97.75
6	(150 °C 90:10)	25.96	85.61	(~100)
7	(150 °C 80:20)	44.03	93.94	(~100)
8	(150 °C 70:30)	40.05	78.89	99.17
9	(150 °C 60:40)	46.50	(~100)	97.44
10	(150 °C 50:50)	40.71	93.97	96.58
11	(140 °C 90:10)	32.62	83.53	96.91
12	(140 °C 80:20)	27.06	74.60	91.03
13	(140 °C 70:30)	30.29	58.41	96.86
14	(140 °C 60:40)	42.92	71.41	95.43
15	(140 °C 50:50)	42.32	71.80	98.43

The weight loss of the hydrolyzed wool fiber-based composites increased smoothly up to the first 30 days due to loss of the cuticular surface morphology of wool fiber and then increased rapidly till 60 and 90 days. Microorganisms in the soil first damage wool scales, and then the cortical cells of wool fibers are susceptible to microbial deterioration by erosion [79]. As shown in Figure 6, after 90 days, both hydrolyzed wool and kraft pulp cellulosic fibers were completely broken off, and the integrity and structure of the fibers had completely collapsed. The results of weight loss and visual appearances by soil degradation are confirmed by SEM images, where the morphology of mixed fiber biocomposites after 60 days of soil burial appeared as a compact matrix fused with the cellulose fibers. The disappearance of the typical structure of the wool fibers in the matrix indicates the degradation of the hydrolyzed wool/kraft pulp biocomposites. One probable reason for this is that soil is a complex system comprising many strains of degrading microorganisms [80]. Another major factor, however, may be the oxidation of fibers in natural soils.

4. Conclusions

In this study, the use of waste biomass such as raw wool that would otherwise be unused or would form a material to be disposed of in a landfill can find its application to produce a biocomposite with the incorporation of kraft pulp. The biocomposite made of kraft pulp/hydrolyzed wool is entirely organic, compostable, and biodegradable, along with a wool modification process that is completely sustainable and green. In the preliminary stage, the biocomposites are pliable and have sufficient mechanical strength for commercial application, as well as a possible thermoregulatory function due to the

wool fibers, which could be beneficial for controlling soil temperatures in agricultural applications and beneficial for special packaging applications. The superheated water hydrolysis treatment used in this study allows adjusting the biodegradation rate and the release of nutrients in the soil. The results show that it is possible to vary the percentage of hydrolyzed wool fibers from 10 to 50% for biocomposite manufacturing. As the amount of hydrolyzed wool fibers in the biocomposites increased, the biocomposites' strength deteriorated. SEM analysis confirms the morphological changes in the raw wool fibers after the hydrolysis, the homogeneity of the biocomposites obtained, and the effect of soil degradation, where wool fibers show a different degree of degradation.

Regarding three superheated water hydrolysis temperatures, 150 °C seems to be the most appropriate for the biocomposite preparation concerning physio-chemical properties of wool and the suitability for wool mixing with cellulose. The FTIR results confirm that the hydrolysis treatment does not result in any new chemical groups or free residues in wool. The weight loss of the hydrolyzed wool fiber-based biocomposites buried in the soil increased smoothly up to the first 30 days due to the cuticular surface loss of wool fiber; after 60 days keratin appeared as a compact matrix fused with the cellulose fibers, and the disappearance of the typical structure of the wool fibers occurred in the matrix, while at the end of 90 days, the integrity and structure of the fibers had completely collapsed. In future studies, the strength characteristics of biocomposites can be improved with the help of binders added during the biocomposites' processing. Moreover, in order to enhance biocomposite performance, many parameters of processes such as refinement, bleaching, bathing, finishing, etc., will be further examined to increase the performance of wool fibers for mainstream applications.

Author Contributions: Conceptualization, P.B. and T.B.; Methodology, P.B. and T.B.; Software, P.B. and G.D.F.; Validation, P.B. and T.B.; Formal Analysis, P.B., M.Z. and A.P.; Investigation, P.B., T.B., G.D.F., M.Z. and A.P.; Resources, M.Z.; Data Curation, P.B.; Writing—Original Draft Preparation, P.B. and G.D.F.; Writing—Review and Editing, P.B., T.B., G.D.F., M.Z. and A.P.; Visualization, P.B. and G.D.F.; Supervision, C.T.; Project Administration, C.T. All authors have read and agreed to the published version of the manuscript.

Institutional Review Board Statement: Not applicable.

Informed Consent Statement: Not applicable.

Data Availability Statement: Not applicable.

Conflicts of Interest: The authors declare no conflict of interest.

References

1. Confederation of European Paper Industries (CEPI). Report on Key Statistics 2019 European Pulp and Paper Industries. Available online: https://www.cepi.org/statistics/ (accessed on 31 August 2021).
2. Packaging Waste Statistics—Eurostat Explained Statistics. Available online: https://ec.europa.eu/eurostat/statistics-explained/index.php?title=Packaging_waste_statistics (accessed on 31 August 2021).
3. Paper & Paperboard Production & Consumption for Europe. Available online: https://paperonweb.com/Europe.htm (accessed on 31 August 2021).
4. Food and Agricultural Organization (FAO). *Yearbook of Forest Products 2010–2014 European Commision*; Food and Agricultural Organization (FAO): Rome, Italy, 2017; p. 186. ISBN 978-92-5-131717-4.
5. El-Sakhawy, M.; Lonnberg, B.; Fahmy, Y.; Ibrahim, A. Organosolv pulping. 3. Ethanol pulping of wheat straw. *Cellul. Chem. Technol.* **1996**, *30*, 161–174.
6. Internal Market, Industry, Entrepreneurship and SMEs Pulp and Paper Industry European Commission. Available online: https://ec.europa.eu/growth/sectors/raw-materials/industries/forest-based/pulp-paper_en (accessed on 31 August 2021).
7. Chandra, R.; Rustgi, R. Biodegradable polymers. *Prog. Polym. Sci.* **1998**, *23*, 1273–1335. [CrossRef]
8. Manda, B.M.K.; Blok, K.; Patel, M.K. Innovations in papermaking: An LCA of printing and writing paper from conventional and high yield pulp. *Sci. Total Environ.* **2012**, *439*, 307–320. [CrossRef]
9. Marrakchi, Z.; Khiari, R.; Oueslati, H.; Mauret, E.; Mhenni, F. Pulping and papermaking properties of Tunisian Alfa stems (*Stipa tenacissima*)—Effects of refining process. *Ind. Crops Prod.* **2011**, *34*, 1572–1582. [CrossRef]

10. Ashraf, M.A.; Zwawi, M.; Taqi Mehran, M.; Kanthasamy, R.; Bahadar, A. Jute Based Bio and Hybrid Composites and Their Applications. *Fibers* **2019**, *7*, 77. [CrossRef]

11. Statista Global Consumption of Paper and Cardboard 2007 to 2018. Available online: https://www.statista.com/statistics/2703 19/consumption-of-paper-and-cardboard-since-2006/ (accessed on 31 August 2021).

12. wbcs Forest Solutions Facts & Trends: Fresh & Recycled Fiber Complementarity Technical Content by ncasi. Available online: https://www.wbcsd.org/Sector-Projects/Forest-Solutions-Group/Resources/Facts-Trends-Fresh-Recycled-Fiber-Complementarity (accessed on 31 August 2021).

13. Fang, G.; Shen, K. Wheat Straw Pulping for Paper and Paperboard Production. In *Global Wheat Production*; IntechOpen: London, UK, 2018.

14. Jha, P.; Sinha, A. Application of Rice-Straw as Raw Material for Production of Handmade Paper. *IPPTA Q. J. Indian Pulp Pap. Tech. Assoc.* **2011**, *23*, 145–148.

15. Mehdikhani, H.; Jalali Torshizi, H.; Dahmardeh Ghalehno, M. Deeper insight into the morphological features of sunflower stalk as Biorefining criteria for sustainable production. *Nord. Pulp Pap. Res. J.* **2019**, *34*, 250–263. [CrossRef]

16. Rainey, T.J.; Covey, G. Pulp and paper production from sugarcane bagasse. In *Sugarcane-Based Biofuels Bioproducts*; John Wiley & Sons, Inc.: Hoboken, NJ, USA, 2016; pp. 259–280.

17. Wan Daud, W.R.; Law, K.N. Oil palm fibers as papermaking material: Potentials and challenges. *Bioresources* **2011**, *6*, 901–917. [CrossRef]

18. García, M.M.; López, F.; Alfaro, A.; Ariza, J.; Tapias, R. The use of Tagasaste (*Chamaecytisus proliferus*) from different origins for biomass and paper production. *Bioresour. Technol.* **2008**, *99*, 3451–3457. [CrossRef] [PubMed]

19. Brix, H.; Ye, S.; Laws, E.A.; Sun, D.; Li, G.; Ding, X.; Yuan, H.; Zhao, G.; Wang, J.; Pei, S. Large-scale management of common reed, Phragmites australis, for paper production: A case study from the Liaohe Delta, China. *Ecol. Eng.* **2014**, *73*, 760–769. [CrossRef]

20. Shatalov, A.A.; Pereira, H. Papermaking fibers from giant reed (*Arundo donax* L.) by advanced ecologically friendly pulping and bleaching technologies. *Bioresources* **2006**, *1*, 45–61.

21. Guha, S.R.D.; Gupta, R.K.; Mathur, G.M.; Sharma, Y.K. Production of Writing and Printing Papers from Prosopis juliflora. *Indian For.* **1970**, *96*, 429–432.

22. Sung, Y.J.; Kim, D.S.; Lee, J.Y.; Seo, Y.B.; Im, C.K.; Gwon, W.O.; Kim, J.D. Application of Conifer Leave Powder to the Papermaking Process as an Organic Filler. *J. Korea Tech. Assoc. Pulp Pap. Ind.* **2014**, *46*, 62–68. [CrossRef]

23. Pirralho, M.; Flores, D.; Sousa, V.B.; Quilhó, T.; Knapic, S.; Pereira, H. Evaluation on paper making potential of nine Eucalyptus species based on wood anatomical features. *Ind. Crops Prod.* **2014**, *54*, 327–334. [CrossRef]

24. Biermann, C.J. Preface to the Second Edition. In *Handbook of Pulping and Papermaking*, 2nd ed.; Academic Press: San Diego, CA, USA, 1996; p. ix. ISBN 978-0-12-097362-0.

25. Ashori, A. Nonwood Fibers—A Potential Source of Raw Material in Papermaking. *Polym.-Plast. Technol. Eng.* **2006**, *45*, 1133–1136. [CrossRef]

26. Mohd Aripin, A. Potential of Non-Wood Fibres for Pulp and Paper-Based Industries. Master's Thesis, Faculty of Science, Technology and Human Development, Universiti Tun Hussein Onn Malaysia, Parit Raja, Malaysia, 2014.

27. EFSA Panel on Animal Health and Welfare (AHAW). Scientific Opinion on the welfare risks related to the farming of sheep for wool, meat and milk production. *EFSA J.* **2014**, *12*, 3933. [CrossRef]

28. Savio, L.; Bosia, D.; Patrucco, A.; Pennacchio, R.; Piccablotto, G.; Thiebat, F. Applications of Building Insulation Products Based on Natural Wool and Hemp Fibers. In *Advances in Natural Fibre Composites, Raw Materials, Processing and Analysis*; Springer: Cham, Switzerland, 2018; pp. 237–247. ISBN 978-3-319-64641-1.

29. Skupin, G.; Blum, R. Method for Producing Filler-Containing Paper Using Biodegradable Polyester Fibers and/or Polyalkylene Carbonate Fibers. WO 2013079378A2, 6 June 2013.

30. Serrano-Ruiz, H.; Martin-Closas, L.; Pelacho, A.M. Biodegradable plastic mulches: Impact on the agricultural biotic environment. *Sci. Total Environ.* **2021**, *750*, 141228. [CrossRef]

31. Espí, E.; Salmerón, A.; Fontecha, A.; García, Y.; Real, A.I. PLastic Films for Agricultural Applications. *J. Plast. Film Sheeting* **2006**, *22*, 85–102. [CrossRef]

32. Le Moine, B.; Ferry, X. Plasticulture: Economy of resources. *Acta Hortic.* **2019**, *1252*, 121–130. [CrossRef]

33. Briassoulis, D.; Giannoulis, A. Evaluation of the functionality of bio-based plastic mulching films. *Polym. Test.* **2018**, *67*, 99–109. [CrossRef]

34. Bhavsar, P.; Patrucco, A.; Montarsolo, A.; Mossotti, R.; Rovero, G.; Giansetti, M.; Tonin, C. Superheated Water Hydrolysis of Waste Wool in a Semi-Industrial Reactor to Obtain Nitrogen Fertilizers. *ACS Sustain. Chem. Eng.* **2016**, *4*, 6722–6731. [CrossRef]

35. *ISO 5264-3:1979: Pulps-Laboratory Beating- Part 3: Jokro Mill Method*; International Organization of Standardization: Geneva, Switzerland, 1979.

36. *ISO 5269-2:2004: Pulps—Preparation of Laboratory Sheets for Physical Testing—Part 2: Rapid-Köthen Method*; International Organization of Standardization: Geneva, Switzerland, 2000.

37. Shogren, R.L. Preparation and characterization of a biodegradable mulch: Paper coated with polymerized vegetable oils. *J. Appl. Polym. Sci.* **1999**, *73*, 2159–2167. [CrossRef]

38. Ning, R.; Liang, J.; Sun, Z.; Liu, X.; Sun, W. Preparation and characterization of black biodegradable mulch films from multiple biomass materials. *Polym. Degrad. Stab.* **2021**, *183*, 109411. [CrossRef]

39. Arshad, K. Biodegradation of Textile Materials. Master's Dissertation, University of Borås, Borås, Sweden, 2011.

40. Tomšič, B.; Simončič, B.; Orel, B.; Vilčnik, A.; Spreizer, H. Biodegradability of cellulose fabric modified by imidazolidinone. *Carbohydr. Polym.* **2007**, *69*, 478–488. [CrossRef]

41. Schweger, B.F.; Kerr, N. Textiles collected during the temporary exhumation of a crew member from the Third Franklin Expedition: Findings and analysis. *J. Int. Inst. Conserv. Can. Group* **1987**, *12*, 9–19.

42. Chen, R. A Study of Cotton Fibers Recovered from a Marine Environment. Ph.D. Dissertation, The Ohio State University, Columbus, OH, USA, 1998.

43. Chen, R.; Jakes, K.A. Cellulolytic Biodegradation of Cotton Fibers from a Deep-Ocean Environment. *J. Am. Inst. Conserv.* **2001**, *40*, 91–103. [CrossRef]

44. Broda, J.; Przybyło, S.; Kobiela-Mendrek, K.; Biniaś, D.; Rom, M.; Grzybowska-Pietras, J.; Laszczak, R. Biodegradation of sheep wool geotextiles. *Int. Biodeterior. Biodegrad.* **2016**, *115*, 31–38. [CrossRef]

45. Jewell, P.A.; Dimbleby, G.W. The Experimental Earthwork on Overton Down, Wiltshire, England: The First Four Years. *Proc. Prehist. Soc.* **1966**, *32*, 313–342. [CrossRef]

46. Peacock, E.E. Biodegradation and characterization of water-degraded archaeological textiles created for conservation research. *Int. Biodeterior. Biodegrad.* **1996**, *38*, 49–59. [CrossRef]

47. Hearle, J.W.S.; Cooke, B.; Lomas, W.D. *Atlas of Fibre Fracture and Damage of Textiles*; Woodhead Publishing Series in Textiles; Woodhead Publishing: Manchester, UK, 1998; ISBN 9781845691271.

48. Hearle, J.W.S. Fracture of common textile fibres. In *Fiber Fracture*; Elices, M., Llorca, J., Eds.; Elsevier Science Ltd.: Oxford, UK, 2002; pp. 329–353. ISBN 978-0-08-044104-7.

49. Huson, M.G. Properties of Wool. In *Handbook of Properties of Textile and Technical Fibres*, 2nd ed.; The Textile Institute; Bunsell, A.R., Ed.; Elsevier: Oxford, UK, 2018; pp. 59–103. ISBN 9780081018866.

50. Wood, T.M.; Phillips, D.R. Another Source of Cellulase. *Nature* **1969**, *222*, 986–987. [CrossRef]

51. Béguin, P.; Aubert, J.P. The biological degradation of cellulose. *FEMS Microbiol. Rev.* **1994**, *13*, 25–58. [CrossRef]

52. Wood, T.M.; McCrae, S.I. Synergism between Enzymes Involved in the Solubilization of Native Cellulose. In *Hydrolysis of Cellulose: Mechanisms of Enzymatic and Acid Catalysis*; Advances in Chemistry; American Chemical Society: Washington, DC, USA, 1979; Volume 181, pp. 10–181. ISBN 9780841204607.

53. Marchisio, V.; Kushwaha, R.; Guarro, J. Keratinophilic fungi: Their role in nature and degradation of keratinic substrates. *Biol. Derm. Other Keratinophilic Fungi* **2000**, *17*, 86–92.

54. Korniłłowicz-Kowalska, T.; Bohacz, J. Biodegradation of keratin waste: Theory and practical aspects. *Waste Manag.* **2011**, *31*, 1689–1701. [CrossRef]

55. DeGaetano, D.H.; Kempton, J.B.; Rowe, W.F. Fungal tunneling of hair from a buried body. *J. Forensic. Sci.* **1992**, *37*, 1048–1054. [CrossRef] [PubMed]

56. Zoccola, M.; Aluigi, A.; Tonin, C. Characterisation of keratin biomass from butchery and wool industry wastes. *J. Mol. Struct.* **2009**, *938*, 35–40. [CrossRef]

57. Tsobkallo, K.; Aksakal, B.; Darvish, D. Analysis of the contribution of the microfibrils and matrix to the deformation processes in wool fibers. *J. Appl. Polym. Sci.* **2012**, *125*, E168–E179. [CrossRef]

58. Tang, H. *Spectroscopy Analysis*; Beijing University Publishing House: Beijing, China, 1992.

59. Sain, M.; Panthapulakkal, S. Bioprocess preparation of wheat straw fibers and their characterization. *Ind. Crops Prod.* **2006**, *23*, 1–8. [CrossRef]

60. Popescu, C.M.; Popescu, M.C.; Singurel, G.; Vasile, C.; Argyropoulos, D.S.; Willfor, S. Spectral Characterization of Eucalyptus Wood. *Appl. Spectrosc.* **2007**, *61*, 1168–1177. [CrossRef]

61. Carrillo, I.; Mendonça, R.T.; Ago, M.; Rojas, O.J. Comparative study of cellulosic components isolated from different Eucalyptus species. *Cellulose* **2018**, *25*, 1011–1029. [CrossRef]

62. Tsuboi, M. Infrared spectrum and crystal structure of cellulose. *J. Polym. Sci.* **1957**, *25*, 159–171. [CrossRef]

63. Jonoobi, M. Chemical composition, crystallinity, and thermal degradation of bleached and unbleached kenaf bast (*Hibiscus cannabinus*) pulp and nanofibers. *Bioresources* **2009**, *4*, 626–639.

64. Kargarzadeh, H.; Ahmad, I.; Abdullah, I.; Dufresne, A.; Zainudin, S.Y.; Sheltami, R.M. Effects of hydrolysis conditions on the morphology, crystallinity, and thermal stability of cellulose nanocrystals extracted from kenaf bast fibers. *Cellulose* **2012**, *19*, 855–866. [CrossRef]

65. Alemdar, A.; Sain, M. Isolation and characterization of nanofibers from agricultural residues—Wheat straw and soy hulls. *Bioresour. Technol.* **2008**, *99*, 1664–1671. [CrossRef] [PubMed]

66. Zhao, X.; Wang, L.; Liu, D.H. Peracetic acid pretreatment of sugarcane bagasse for enzymatic hydrolysis: A continued work. *J. Chem. Technol. Biotechnol.* **2008**, *83*, 950–956. [CrossRef]

67. Li, R.; Fei, J.; Cai, Y.; Li, Y.; Feng, J.; Yao, J. Cellulose whiskers extracted from mulberry: A novel biomass production. *Carbohydr. Polym.* **2009**, *76*, 94–99. [CrossRef]

68. Li, L.; Frey, M.; Browning, K.J. Biodegradability Study on Cotton and Polyester Fabrics. *J. Eng. Fiber. Fabr.* **2010**, *5*, 155892501000500400. [CrossRef]

69. Spence, E.E. *Encyclopedia of Polymer Science and Technology*, 2nd ed.; Wily-Interscience: New York, NY, USA, 1987; Volume 10.

70. Levy, I.; Nussinovitch, A.; Shpigel, E.; Shoseyov, O. Recombinant cellulose crosslinking protein: A novel paper-modification biomaterial. *Cellulose* **2002**, *9*, 91–98. [CrossRef]

71. Xu, G.G.; Yang, C.Q.X. Comparison of the kraft paper crosslinked by polymeric carboxylic acids of large and small molecular sizes: Dry and wet performance. *J. Appl. Polym. Sci.* **1999**, *74*, 907–912. [CrossRef]

72. Vineis, C.; Aluigi, A.; Tonin, C. Outstanding traits and thermal behaviour for the identification of speciality animal fibres. *Text. Res. J.* **2010**, *81*, 264–272. [CrossRef]

73. Fortunati, E.; Aluigi, A.; Armentano, I.; Morena, F.; Emiliani, C.; Martino, S.; Santulli, C.; Torre, L.; Kenny, J.M.; Puglia, D. Keratins extracted from Merino wool and Brown Alpaca fibres: Thermal, mechanical and biological properties of PLLA based biocomposites. *Mater. Sci. Eng. C* **2015**, *47*, 394–406. [CrossRef]

74. Eslahi, N.; Dadashian, F.; Nejad, N.H. Optimization of enzymatic hydrolysis of wool fibers for nanoparticles production using response surface methodology. *Adv. Powder Technol.* **2013**, *24*, 416–426. [CrossRef]

75. Dalla Fontana, G.; Varesano, A.; Vineis, C. Effect of the Bleaching on Physical and Mechanical Properties of Different Fabrics. *Fibers Polym.* **2018**, *19*, 2590–2596. [CrossRef]

76. Ibrahim, S.; El-Amoudy, E.; Shady, K.E. Thermal Analysis and Characterization of Some Cellulosic Fabrics Dyed by a New Natural Dye and Mordanted with Different Mordants. *Int. J. Chem.* **2011**, *3*, 40–54. [CrossRef]

77. Yang, H.; Yan, R.; Chen, H.; Lee, D.H.; Zheng, C. Characteristics of hemicellulose, cellulose and lignin pyrolysis. *Fuel* **2007**, *86*, 1781–1788. [CrossRef]

78. Bradbury, J.H.; Chapman, G.V.; King, N.L.R. The Chemical Composition of Wool II. Analysis of the Major Histological Components Produced by Ultrasonic Disintegration. *Aust. J. Biol. Sci.* **1965**, *18*, 353–364. [CrossRef] [PubMed]

79. Sun, Y.; Luo, J.; Ni, A.; Bi, Y.; Yu, W. Study on Biodegradability of Wool and PLA Fibers in Natural Soil and Aqueous Medium. *Adv. Mater. Res.* **2013**, *641–642*, 82–86. [CrossRef]

80. Guo, W.; Tao, J.; Yang, C.; Zhao, Q.; Song, C.; Wang, S. The rapid evaluation of material biodegradability using an improved ISO 14852 method with a microbial community. *Polym. Test.* **2010**, *29*, 832–839. [CrossRef]